Characterization of Asphaltenes Aggregation and Fragmentation in a Shear Field

Nazmul H. G. Rahmani and Jacob H. Masliyah
Dept. of Chemical and Materials Engineering, University of Alberta, Edmonton, Alberta, Canada T6G 2G6

Tadeusz Dabros
CANMET, Devon, Alberta, Canada T9G 1A8

Aggregation and breakup of asphaltenes flocs in a Couette flow device are studied for various values of shear rate (G), volume fraction of particles (φ), and solvent composition (ratio of toluene to n-heptane in the solution X_s). The number average asphaltene aggregate size initially increases before achieving a maximum size and then decreases until reaching a steady-state value that reflects a balance between aggregation and fragmentation. Increasing the applied shear rate leads to higher aggregation and fragmentation rates, reducing the steady-state average aggregate size and the characteristic relaxation time required to achieve a steady state. For a fixed value of G, when either φ is increased or X_s is decreased, the steady-state floc size increases. The kinetics of the aggregation-fragmentation process and the attainment of steady state by asphaltenes aggregates were modeled using a population balance approach. The model describes the time evolution of the average floc size using fitted parameters (the breakup coefficient for shear fragmentation, b and the porosity of the aggregates ϵ). Binary breakage was included in calculations and collision efficiency was assumed to be equal to one.

Introduction

Petroleum asphaltenes have been a subject of extensive research. On the basis of solubility, asphaltenes are defined as the part of petroleum that is insoluble in *n*-alkanes and completely miscible in aromatic hydrocarbons such as toluene or benzene (Speight, 1990). This property is used for the extraction of asphaltenes. The above definition is in some sense arbitrary, as the molecular structure of asphaltenes varies significantly depending on their origin, method of oil recovery, and history of extraction (Burya et al., 2001). According to chemical structure, asphaltenes are aromatic multicyclic molecules surrounded and linked by aliphatic chains and heteroatoms; published molar mass data for petroleum asphaltenes range from 500 g/mol to a high of 50,000 g/mol (Long, 1981). The polarity and complex structure of asphaltenes lead to their self-association, flocculation, and precipitation during the course of heavy oil processing.

On the one hand, the importance of asphaltenes in the petroleum industry is through its negative impact on various petroleum operations, such as exploration, production, transportation, and refining (Yen and Chilingarian, 1994; Sheu and Storm, 1995). For example, upon release of a well pressure, asphaltenes may precipitate and plug the reservoir formation and well bore. On the other hand, a new technology is under development for cleanup operation of bitumen originating from the shallow oil sands deposits in northern Alberta, which takes advantage of asphaltenes propensity to aggregate. Asphaltenes, a high molecular weight constituent of bitumen, when precipitated out of a bitumen/light aliphatic hydrocarbon mixture, act as flocculent to the emulsified water droplets and fine solids. Very little is known about the mechanical properties (such as structure and yield strength) of the precipitated asphaltene aggregates. This article focuses on determining these properties under dynamic conditions. The size range of studied aggregates is similar to the ones encountered in commercial systems as reported by Long et al. (2002).

Correspondence concerning this article should be addressed to J. H. Masliyah.

The formation of colloidal asphaltenes associates in several organic solvents and in crude oil was observed for the first time more than half a century ago (Mack, 1932; Pfeiffer and Saal, 1940). It is postulated that, in aromatic solvents, asphaltenes can form micelle-like aggregates above a certain concentration, known as the critical micelle concentration (CMC). The CMC data for asphaltenes in toluene have been determined using a variety of methods, such as the measurement of surface tension (Rogacheva et al., 1980) and calorimetric titration (Andersen and Birdi, 1991; Sheu et al., 1992). The values obtained by various authors differ widely (such as the CMC in toluene is in the range from 0.10 to 3.24 gL^{-1}). This can be explained by the diversity of the techniques applied and by the variety of asphaltenes (origin, extraction, impurities) studied. Sheu and Storm (1995) have noted that asphaltenes in a good solvent below the CMC are in a molecular state, whereas, above the CMC, asphaltene micelle formation occurs in a manner similar to that in surfactant systems, but with less uniformity in their structure and with more polydispersity. According to other investigations, the structure and the shape of asphaltenic micelle-like associates appear to be much more complicated than that of classic surfactant micelles (Drushel and Schultz, 1980, Yudin et al., 1998). These studies indicate that asphaltene micelle-like associates are formed as a result of multiple interactions: aggregates about 2–5 nm in size are present either in a molecular form or are formed by strong intermolecular attraction forces, while the larger particles are self-associates, formed from these small aggregates by weaker attraction forces.

Although many studies have been conducted on the growth of colloidal asphaltene particles in hydrocarbon solutions, the flocculation of asphaltene particles under hydrodynamic shear flow has not been investigated. It bears a valuable implication in industrial applications. The objective of the present work is to study the kinetics of aggregation of suspended "primary" particles of asphaltenes under controlled shear conditions. A mixture of toluene and *n*-heptane is often used to investigate the stability and the precipitation process of asphaltenes. At a certain threshold value of the ratio of *n*-heptane to toluene, the asphaltenes in solution becomes unstable and asphaltenes particles start to precipitate. It is found that when a concentrated solution of asphaltenes in toluene is added to excess heptane, the precipitated asphaltene grows from sub-micron-size primary particles to aggregates that are orders of magnitude larger within a few minutes.

In the present study, the growth of the asphaltenes flocs takes place in a well-controlled, laminar shear flow of a Couette device. Image analysis is used to measure the size of the aggregates in suspension. This article is a first step to study asphaltene flocculation for a model system using optical microscopy. It presents both experimental and theoretical studies of dynamics of aggregation and fragmentation for asphaltene particles under shear in an organic solvent. The growth of the aggregates is investigated as a function of shear rate, ratio of toluene to *n*-heptane, and asphaltenes concentration. It is shown how the variation in the applied shear rate leads to the change of parameters of a steady-state average aggregate size and the characteristic relaxation time required to achieve the steady-state. A population balance approach is used to shed light on the effect of G, φ, and X_s in the aggregation and fragmentation processes. The model, developed in this work, describes well and explains the experimental observations and has two adjustable parameters: the porosity of the aggregates ϵ and the breakup coefficient for shear fragmentation b. The values obtained for these two parameters are discussed. The microscopic technique described in this article is ideally suited for the study of suspensions containing solid asphaltenes particles in the sub-micron size range, which flocculate to form aggregates several microns in diameter. The technique also provides information on aggregation kinetics and aggregate size.

Population Balance Model

Theory

Since the pioneering work of Smoluchowski (1917), the physical processes that control kinetics of particle aggregation have been quite well known. The aggregation rate depends upon the rate at which collisions occur and on the probability of cohesion of particles during a collision. However, the fragmentation processes are not so well understood. The main objective of this work is to establish a population balance model that describes the kinetics of aggregation and fragmentation of asphaltenes particles.

During the initial stages of shear-induced aggregation, particle growth is dominant and the average floc size increases rapidly. As the flocs grow and hydrodynamic stresses become of the order of the yield stress of the aggregates, the fragmentation becomes significant. To model the rate of change of size of particles of a given size due to the processes of aggregation and fragmentation, Austin (1971) and Friedlander (1977) proposed the following expression

$$\frac{dn_i}{dt} = \frac{1}{2}\sum_{j+k=i} \alpha\beta_{jk}(V_j,V_k)n_j n_k - n_i \sum_{k=1}^{n_{\max}} \alpha\beta_{ki}(V_k,V_i)n_k - B_i n_i + \sum_{j=i+1}^{n_{\max}} \gamma_{i,j} B_j n_j \quad (1)$$

where n_i is the number concentration of flocs of size i (meaning that a single floc contains i primary particles), α is the collision efficiency or the fraction of collisions that result in aggregation, and β_{jk} is the collision frequency for particles of volume V_j and V_k. B_i is the fragmentation or breakup rate of flocs of size i, and $\gamma_{i,j}$ is the breakup distribution function defining the volume fraction of the fragments of size i originating from j-sized particles. Here, the index $n_{\max}$ represents the largest particle size that will form fragments of size i upon breakup.

The first term on the righthand side of Eq. 1 represents the formation of particles of size i by collisions of smaller j- and k-sized particles. The second term on the righthand side denotes the loss of particles of size i by collisions with particles of any other size. The third term on the righthand side describes the loss of particles of size i by fragmentation and the fourth term on the righthand side defines the formation of particles of size i by the fragmentation of larger particles.

The growth of aggregates occurs over a wide size range, so a discrete model of flocculation may require excessive computation time (Landgrebe and Pratsinis, 1990). The size do-

main considered is divided into ranges or bins to ease computation. Equations describing the particle number concentration within each bin are used. Each bin is represented by an characteristic volume V_i that is the average volume of the sizes contained in the section

$$V_i = \frac{u_{i-1} + u_i}{2} \tag{2}$$

where u_i is the upper boundary volume of bin i and u_{i-1} is the lower boundary volume. V_i is also a function of the previous section V_{i-1}

$$V_i = \frac{fV_{i-1}}{1-\epsilon} \tag{3}$$

where f is the sectional spacing and ϵ is the porosity of aggregates. In this study, a numerical technique is used to simulate the evolution of the particle size with $f = 2$ (Hounslow et al., 1988; Kusters et al., 1993; Spicer and Pratsinis, 1996), and for this specific case, Eq. 1 can be rewritten as

$$\frac{dN_i}{dt} = \sum_{j=1}^{i-2} 2^{j-i+1}\alpha\beta_{i-1,j}N_{i-1}N_j + \frac{1}{2}\alpha\beta_{i-1,i-1}N_{i-1}^2 - N_i\sum_{j=1}^{i-1} 2^{j-i}\alpha\beta_{i,j}N_j - N_i\sum_{j=i}^{i_{\max}} \alpha\beta_{i,j}N_j - B_iN_i + \sum_{j=i+1}^{i_{\max}} \Gamma_{i,j}B_jN_j \tag{4}$$

where $\Gamma_{i,j}$ is the breakup distribution function from Eq. 1 modified to conserve volume within the framework of the sectional mode for the particular case of $f = 2$, and N_i is the number concentration of aggregates having characteristic volume V_i. Calculations are carried out using 31 sections, from $i = 1$ to $i_{\max} = 31$. In order to represent the whole population of particles, the number of equations that needs to be solved is the same as the number of classes or sections. Volume conservation has been enforced in the model, which means that when a particle of size class i aggregates with a particle of size class j, a particle of size class k is formed whose volume is

$$V_k = V_i + V_j \tag{5}$$

The minimum size corresponds to the smallest particle size (that is, the size of the primary particle) observed in experiments at the early stage (Oles, 1992; Kusters et al., 1993).

Closure of Model Parameters and Description of Model

Collision efficiency (α)

According to the Smoluchowski model, the colloidal particles in the flow field are assumed to follow the fluid streamlines and collide with each other when the distance between the streamlines is less than the sum of the particle radii (Masliyah, 1994). However, during a collision between two particles, the particles experience hydrodynamic and repulsive or attractive colloidal forces. Taking these forces into account, a factor is introduced, called the orthokinetic collision efficiency α that represents the ratio of actual aggregation rate to Smoluchowski's aggregation rate. Many authors (Mishra et al., 1998; Mousa and van de Ven, 1991) have expressed this factor as a stability ratio W which is merely the reciprocal of α. For aggregation in a shear field, Smoluchowski's rate was derived by neglecting Brownian motion, gravitation effects, colloidal forces, and hydrodynamic interactions.

In the present calculations, collision efficiency was assumed to be equal to 1 ($\alpha = 1$). A similar assumption was also made by Spicer and Pratsinis (1996) and Serra and Casamitjana (1998), and can be justified by the fact that large colloidal aggregates have fractal structures. As was pointed out by Jiang and Logan (1991), a higher aggregation frequency exists due to the fractal nature of the actual flocs. Hence, a higher value of the collision frequency (β) may compensate for the reduction in the collision efficiency (α) and, consequently, the product of α and β takes care of the inherent inadequacy of this assumption. However, it is important to point out that α is a complex function of the surface properties of the particles, the structure of the aggregates or the diameter of the aggregates, hydrodynamic effects, and the prevailing colloidal forces (Burban et al., 1989). Various expressions exist relating α to system variables such as ionic strength and viscous retardation of collisions (Higashitani et al., 1982; Han and Lawler, 1992). However, these expressions are not applicable for the present study, since it deals with organic solvents and a laminar flow regime.

Collision frequency ($\beta_{i,j}$)

Particles in the liquid medium may collide due to three different processes: Brownian motion, fluid shear, and differential settling (Elimelech et al., 1995). The collision frequency function due to Brownian motion is

$$\beta_{i,j} = \frac{2}{3}\frac{k_BT}{\mu}\frac{(d_i + d_j)^2}{d_id_j} \tag{6}$$

The collision frequency function due to fluid shear is

$$\beta_{i,j} = \frac{G}{6}(d_i + d_j)^3 \tag{7}$$

The collision frequency function due to differential settling is

$$\beta_{i,j} = \frac{\pi g}{72\mu}(d_i + d_j)^2|\Delta\rho_i d_i^2 - \Delta\rho_j d_j^2| \tag{8}$$

where g is the acceleration due to gravity and $\Delta\rho_i = \rho_i - \rho$ is the difference between the effective density of the particle of size class i and the density of the liquid medium.

Han and Lawler (1992) observed that for both orthokinetic aggregation and differential sedimentation, the collision fre-

quency was a strong function of particle size, dominated by the diameter of the larger of the two particles. The authors extended the analysis to compare collisions between all pairs of particles with sizes in the range 1–1,000 μm. For a range of values of G, the authors found that differential sedimentation was dominant only when one particle was quite large and the other was significantly smaller. In all other cases, orthokinetic aggregation was the dominant mechanism. For the present study, the orthokinetic collision frequency (Eq. 7) was used for the calculations.

Fragmentation rate (B_i)

The fragmentation of aggregates is caused by hydrodynamic stresses. The most common breakage mechanisms are: (a) erosion of primary particles or small fragments from the floc surface; (b) "bulgy deformation," rupture, or splitting of the floc (Pandya and Spielman, 1982; Chen et al., 1990). Erosion releases loosely bound particles from the surface of the aggregate. The splitting mechanism arises from pressure differences on the opposite sides of the floc that induce a shearing type of fragmentation (Parker et al., 1972). The larger an aggregate becomes, the more susceptible it is to breakage. The fragmentation rate is given as a function of particle volume by Kapur (1972)

$$B_i = bV_i^a \tag{9}$$

where $a = 1/3$. This is consistent with the theoretical expectation that breakup rate is proportional to floc diameter (Boadway, 1978) and b is the breakup rate coefficient for shear-induced fragmentation (Pandya and Spielman, 1982)

$$b = b'G^y \tag{10}$$

where y is a constant inversely proportional to the floc strength and b' is a proportionality constant that is determined from data fitting. This type of power law relationship between aggregate size and shear rate is commonly used to correlate experimental (Parker et al., 1972) and simulation results (Chen et al., 1990).

Breakup distribution function ($\Gamma_{i,j}$)

Different types of breakup distribution functions ($\Gamma_{i,j}$) can be assumed for the sectional description of aggregation and fragmentation. Here, a binary breakage function is examined that describes the breakup of an aggregate into two parts of equal size (Chen et al., 1990)

$$\Gamma_{i,j} = \frac{V_j}{V_i}\text{; binary breakage, so } j = i+1 \tag{11}$$

The expression for $\Gamma_{i,j}$ in Eq. 11 is only valid for f being equal to 2. All the breakage parameters in this model best describe fragmentation by splitting. Although splitting is energetically less likely, the velocity fluctuations lead to a pressure gradient across the floc making the splitting mode more significant than erosion.

Porosity of the aggregates (ϵ)

Substantial research indicates that flocs formed by aggregation may have a fractal structure. Unlike fractals with an increasing porosity as their size increases, Euclidean objects have a constant porosity (Meakin, 1988; Jiang and Logan, 1991; Gregory, 1997). Since fractal structure was not incorporated in the model, a constant porosity (ϵ) is assumed for aggregate formation from primary particles. For an aggregate made up of n spherical primary particles each of volume V_1, the porosity can be derived as

$$\epsilon = 1 - \frac{nV_1}{V_a} \tag{12}$$

where V_a is the aggregate volume. In this model, the porosity of the aggregates ϵ is used as an adjustable parameter and it can be expressed as

$$\epsilon = -aG + c \tag{13}$$

where a and c are proportionality constants that are determined from data fitting. This type of linear relationship between aggregate porosity and shear rate can be used to correlate experimental and simulation results.

Equations 3, 7, 9–11, and 13 provide closure to the population balance equation. They were substituted into Eq. 4 and the sectional model was solved numerically by a finite difference scheme using RK15s, an ordinary differential equation solver.

Experimental Method

Materials

Asphaltenes used in this study are derived from Syncrude Coker feed Athabasca bitumen (bitumen that has been treated to remove most of the solids and water and is ready for upgrading). However, it still contains mineral solids, which make up about 1 wt. % of the bitumen. The "solids," which include fine clays, are insoluble in toluene (Yarranton, 1997). To remove the solids, the bitumen is first dissolved in toluene and centrifuged at 35,000 g for 30 min. The supernatant liquid is recovered and evaporated until only dry, solids-free bitumen remains. Asphaltenes are extracted from this bitumen with a 40:1 volume ratio of heptane to bitumen (solids-free). The mixture is stirred for 4 h and left standing to allow the precipitated asphaltenes to settle overnight. Then, the supernatant liquid is removed and the remaining precipitate is further diluted with heptane at a 4:1 volume ratio of heptane to asphaltene. After 4 h, the final mixture is filtered using 0.22 μm Millipore filter paper and the remaining asphaltenes are washed thoroughly with heptane until the filtrate (heptane) becomes colorless. The precipitated asphaltenes are dried in a vacuum oven dryer at 23 kPa absolute pressure and 50°C. The drying process usually requires one week. The asphaltenes recovered in this method make up about 16 wt. % of original bitumen.

Reagent-grade toluene and heptane were purchased from Fisher Scientific.

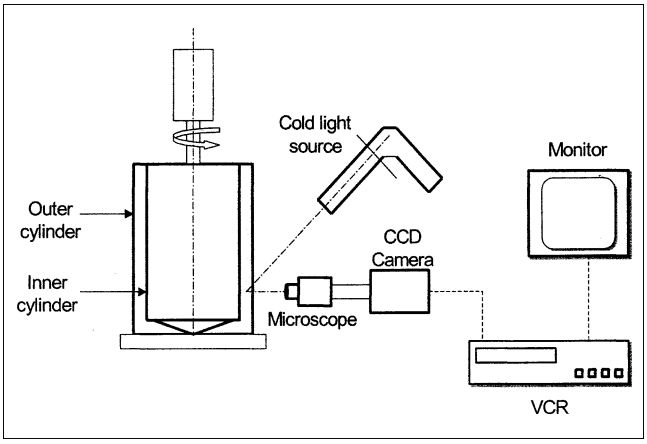

Figure 1. Experimental setup.

Apparatus

The Couette device (where the asphaltenes-solvent mixture is introduced) is shown in Figure 1. This type of apparatus is used, because, under certain conditions, it generates a well-defined shear field. Couette flow is preferable, because, if $h \ll d$ (where d is the inner Couette diameter and h is the gap width), a constant velocity gradient across the gap is achieved (Cummins et al., 1990). In a turbulent flow regime, Couette flow generates a more isotropic turbulence than other flow schemes such as blades in a jar (Pandya and Spielman, 1982).

The inner cylinder, with a diameter of 50 mm, is made of Teflon to provide better optical reflection. The outer cylinder, with an inner diameter of 60 mm, is made of Pyrex glass to allow the mixture to be observed. The height of the cylinders is 200 mm, and the annular gap between them is 5 mm. For the second and third sets of experiments (as shown in Table 1), the height of the cylinders is doubled to 400 mm, but the annular gap between them remains the same (5 mm). The outer cylinder is fixed, while the rotational speed of the inner cylinder can be adjusted. For all three sets of experiments, the location of the observation area or control volume is 50 mm above the bottom of the cylinder. Images of asphaltenes aggregates in suspension are obtained using a microscope (Carl Zeiss Canada Ltd.) coupled with a CCD camera and a video recorder. Image analysis software (Sigma ScanPro 4) is used to calculate the geometrical properties of the aggregates from the captured images.

Sample Preparation

Tests at different shear rates

Initially, a 10.0 mg sample of asphaltenes is dissolved in 10.0 mL of toluene. The solution is added to 150 mL of *n*-heptane in a beaker and is stirred instantly at 300 rpm with a marine propeller for 15 s to ensure complete mixing of the solution. Although no baffle is placed in the beaker, aeration and evaporation of the solvent can be neglected due to low mixing intensity and short mixing time. Following the mixing, the asphaltenes solution is transferred into the outer glass cylinder, which is quickly snapped into the Couette device, and the rotation of the inner cylinder begins at a fixed rpm. This is considered as the starting time for aggregation. The experiments are carried out at a constant shear rate (G) ranging from 1.2 to 12.7 s^{-1}. Because of the limited optical resolution, the fine asphaltenes aggregates and structural details of particles became visible when they reached approximately 30 μm. Hence, there is a time lag before the images can be captured due to lack of growth of the asphaltenes flocs to observable size (Figure 2).

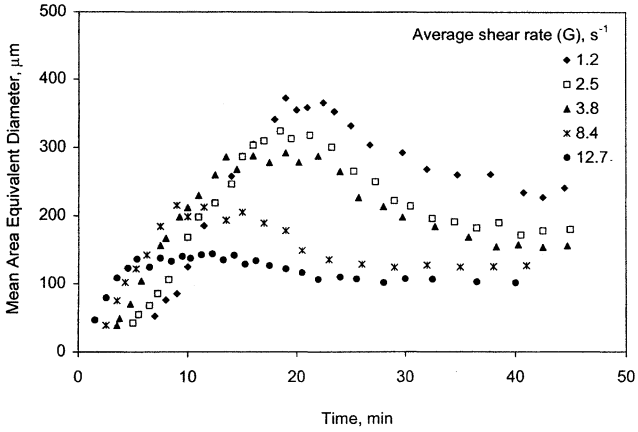

Figure 2. Growth kinetics of asphaltene aggregates under shear at toluene to heptane solvent ratio of 1:15 and particle concentration of 12.8 mg/L.

Table 1. Amount of Precipitated Asphaltenes, Particle Volume Fraction, and Asphaltenes Concentration in Solution for Different Experimental Conditions

Avg. Shear Rate, G (s^{-1})	Ratio of Toluene to *n*-Heptane in Solution	Init. Conc. of Asphaltenes in Toluene (mg/L)	Init. Conc. of Asphaltenes in Toluene + *n*-Heptane Mixture (mg/L)	Final Amount of Precipitated Asphaltenes (mg)	Asphaltenes Particle Conc. in Toluene + *n*-Heptane Mixture (mg/L)	Asphaltenes Particle Volume Fraction $\phi(10^{-6})$
1.2–12.7	1:15	1,000	62.5	4.1 ± 0.4	12.8	10.81
2.5	1:15	1,000	62.5	4.1 ± 0.4	12.8	10.81
2.5	1:7	1,000	62.5	3.3 ± 0.3	10.3	8.60
2.5	1:3	1,000	62.5	2.8 ± 0.2	8.8	7.29
2.5	1:7	1,000	62.5	3.3 ± 0.3	10.3	8.60
2.5	1:7	750	46.9	1.7 ± 0.2	5.3	4.43
2.5	1:7	500	31.3	1.3 ± 0.2	4.1	3.38

Although the initial asphaltenes feed concentration was 62.5 mg/L, the amount of precipitated asphaltenes at the end of the experimental run was found to be significantly less than the initial amount added. After the stirring is stopped, the asphaltenes aggregates are allowed to settle out of solution. The precipitated asphaltenes aggregates are filtered using 0.22-micron Millipore filter article. Since these aggregates are weak or fragile, great care must be taken in the measurement and handling of the flocs. The precipitate is then dried in a vacuum dryer at 23 kPa absolute pressure and room temperature until the weight becomes constant. The asphaltenes recovered by this method is the precipitated amount and is used to calculate the particle volume fraction in solution assuming a specific gravity of 1.20 for solid asphaltenes (Yarranton, 1997). However, the actual volume of the precipitate is larger due to the porous structure of the asphaltene aggregates. It means that the density of the aggregates is lower than 1.2 g/cm^3.

Tests at different solvent compositions and asphaltene particle concentrations

Table 1 shows the amount of precipitated asphaltenes, particle volume fraction (ϕ), and asphaltenes particle concentration in the solution for all experiments carried out at different conditions (set 1 to 3). From this table, it can be seen that the second set of experiments were carried out at a constant shear rate of 2.5 s^{-1} and an initial asphaltenes concentration of 62.5 mg/L, but the solvent composition (the ratio of toluene to heptane in the solution) varied. In the third set of experiments, the shear rate was set at 2.5 s^{-1}, and the ratio of toluene to *n*-heptane was kept fixed at 1:7; the initial asphaltenes concentration varied from 62.5 mg/L to 31.3 mg/L.

Results and Discussion

Effect of shear on the growth of asphaltene flocs

Figure 2 shows the kinetics of asphaltenes growth in terms of the aggregate size as a function of time for a given shear rate. The number mean diameter D_n derived from the aggregate projected area, can be defined as follows

$$D_n = \frac{\sum_{i=1}^{i=k} n_i D_i}{\sum_{i=1}^{i=k} n_i} \tag{14}$$

where D_n is a function of time, n_i is the number of particles measured in size range i, D_i is the middle of class range i size, and k is the number of particle-size ranges. The number mean diameter is a good parameter to represent the complete growth process in image analysis and is used as the characteristic size.

Different shear rates (G) are used in the range of 1.2–12.7 s^{-1}. A characteristic time-dependent behavior is found for all experiments. For all values of G, the aggregate size increases rapidly with time, consistent with the results of previous experimental studies (Oles, 1992; Spicer and Pratsinis, 1996). As explained earlier, due to the limited resolution of the microscope-camera system, particles with size around 30 μm will be considered to be the "primary" particles from which aggregation starts. The size and concentration of primary particles also defines our initial conditions for the population balance.

As shown in Figure 2, the growth of the polydispersed asphaltenes primary particles in the suspension appears to be a strong function of the shear rate. The rate of growth of the flocs is greater at higher shear, which can explain the earlier appearance of primary flocs of the same size, about 30 μm, at the higher shear, as well as by the slight change in the slopes of the size vs. time curves. As the shear rate is increased, the collision rate increases. Consequently, the aggregate mean size increases more rapidly and the slopes become steeper. For shear rates higher than 8.4 s^{-1}, not much growth is observed. At times greater than 10 to 25 min (depending on the shear rate), the aggregates pass through a maximum size. During the growth phase of the flocs, as the concentration of large flocs increases, breakup becomes more significant. In addition, it is found that the system reaches maximum size state more rapidly when the shear rate is increased, with the size of the aggregates being smaller. This suggests

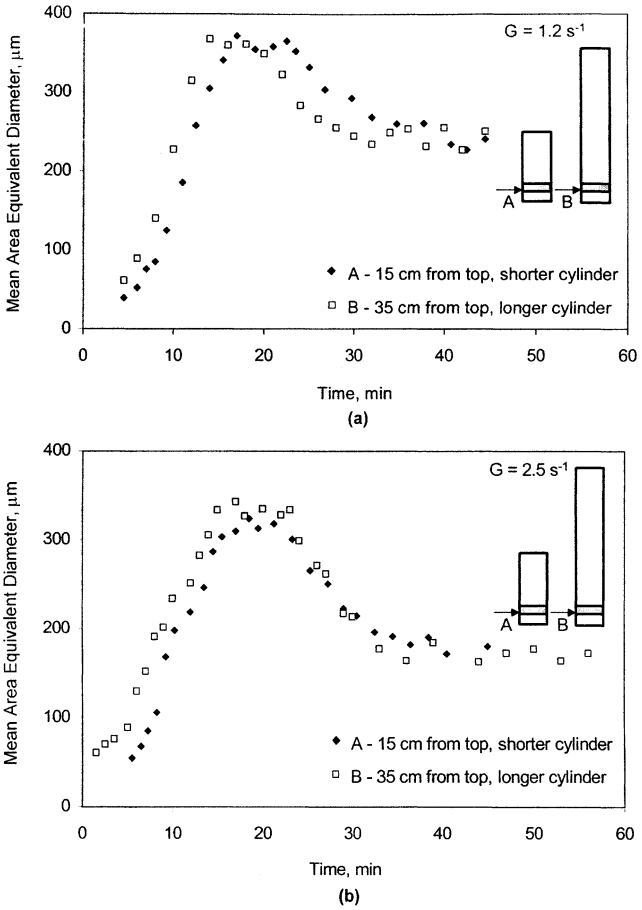

Figure 3. Growth kinetics comparison between different observation locations at toluene:heptane = 1:15, and asphaltene particle concentration = 12.8 mg/L.

In Figure 3a, $G = 1.2$ s^{-1}, and in 3(b), $G = 2.5$ s^{-1}.

that, as the shear rate is increased, the flocs become more likely to break due to the hydrodynamic shear force. Similar behavior is supported by other studies, such as Burban et al. (1989), Oles (1992), Spicer and Pratsinis (1996), and Serra and Casamitjana (1998). After this stage, the mean aggregate size starts to decline until it reaches a steady-state size. However, this behavior was initially thought to be a mere artifact due to differential settling of the flocs beyond these times. In such a case, since the flocs are denser than the liquid medium, the larger flocs would settle out of the observation region after a certain time, leaving only the smaller aggregates. In order to test this hypothesis, the cylinders in the Couette device were made twice as long. If the rates of aggregation and fragmentation become equal after the flocs attain the maximum size, the longer cylinder should provide a broader maximum size plateau before the observed size would start declining solely due to settling. However, if a similar curve is found as that in Figure 2, it should prove that aggregation is overtaken by fragmentation or, possibly, restructuring.

In Figures 3a and 3b, the mean aggregate size as a function of time is shown for the two cylinders under the same experimental conditions, that is, shear rate, asphaltenes particle concentration, and toluene-to-heptane ratio in the solution are kept the same. The mean aggregate size variations with time are found to be similar when the observation points are located 15 cm (200-mm cylinder) and 35 cm (400-mm cylinder) below the top surface in the cylinders. This means that, regardless of where the measurements are taken, what is observed is the net result of breakup-restructuring and aggregation, and not due to settling. Hence, the observed maximum in aggregate size is not an artifact of the experimental apparatus. The maximum in the aggregate size can be explained as a result of restructuring of the large flocs produced initially to form more compact structures. Under constant shearing, large open flocs become more compact as the flocs restructure or fragment and reform more durable structures (Bouyer et al., 2001; Spicer et al., 1996).

Effect of asphaltenes particle concentration on floc growth

Figure 4 shows the effect of particle concentration on the growth of asphaltenes flocs. All three experiments are carried out at a shear rate of 2.5 s^{-1} and toluene-to-heptane ratio of 1:7. It can be observed from the figure that a higher particle concentration provides a smaller relaxation time for visible floc formation and increases the initial aggregation rate (observed from the initial slopes of the curves) by decreasing the average distance between particles, thus reducing the characteristic time between collisions. The dynamic balance between the floc growth and breakage determines the average floc size that is attained at steady state. Increasing ϕ leads to an increase in the aggregation rate to a much greater extent than the fragmentation rate and, consequently, a larger steady-state floc size is reached. However, no significant difference in steady-state floc size is observed for asphaltenes particle concentrations of 5.3 and 4.1 mg/L. A larger ϕ also results in a faster attainment of the maximum floc size than at lower asphaltene concentrations, because of the accelerated kinetics of both aggregation and fragmentation.

Yudin et al. (1998) investigated the kinetics of asphaltene aggregation in toluene and *n*-heptane mixtures with dynamic

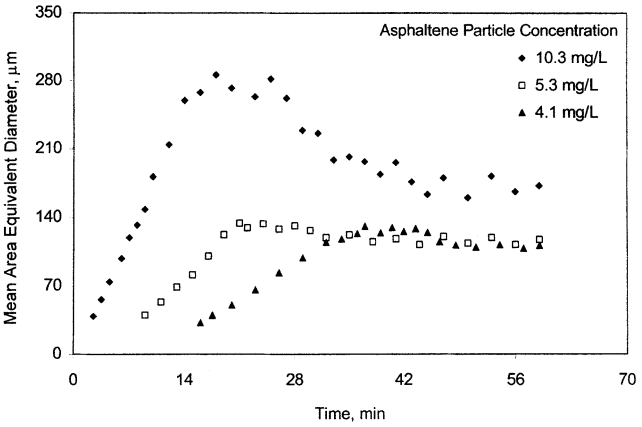

Figure 4. Evolution of average aggregate diameter vs. time at different concentrations of asphaltene particles and at $G = 2.5\ s^{-1}$.

light scattering. They reported a CMC value of about 3 g/L for asphaltenes in toluene and varied the concentration of asphaltenes in toluene from 1 to 10 g/L. The aggregation kinetics was measured upon adding the near precipitation threshold concentration of *n*-heptane. Two types of kinetic behaviors were observed. The noted size range for asphaltene aggregates was less than 5 microns. At a concentration of asphaltenes in toluene lower than the CMC, the aggregates were formed from "asphaltene molecules" and the character of the aggregation was solely determined by diffusion-limited aggregation (DLA). Above the CMC, the aggregates were formed from micelles and reaction-limited aggregation (RLA) took place at least in the initial stage of particle growth. As the asphaltene concentration increased, the micelles became larger and the potential barrier became higher. That is why the RLA rate slowed down with increasing asphaltene concentration, which was exactly opposite of the DLA process.

In the present study all asphaltene solutions in toluene are dilute, less than 1 g/L, that is, well below the CMC. Similarly, as in the case of the DLA process, higher aggregation rate and larger floc size are observed for higher asphaltene concentrations. Under the present conditions, an excess of heptane is added to destabilize the system. Therefore, the kinetics is governed by hydrodynamic shear-induced aggregation.

Effect of solvent composition on the growth of asphaltenes flocs

Figure 5 represents the effect of the ratio of toluene to *n*-heptane in the solution on the growth rate of asphaltenes flocs. The shear rate was set at 2.5 s^{-1}, and the initial asphaltenes particle concentration was 62.5 mg/L for all experiments. A lower ratio of toluene to *n*-heptane means lower solubility of asphaltenes and, accordingly, greater quantities of precipitated asphaltenes are observed at the end of an experiment. The amount of precipitate, which is always significantly less than the initial amount added to the solution, is used to determine the particle concentration in the solution (Table 1). Hence, a lower toluene-to-heptane ratio results in

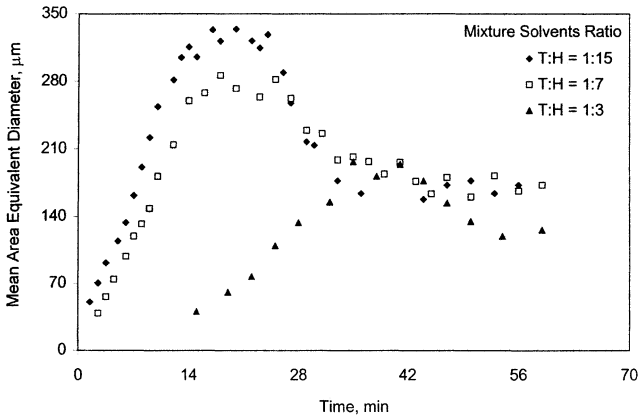

Figure 5. Evolution of average aggregate diameter vs. time at different toluene to heptane ratios in the solution (X_s) and at $G = 2.5\ s^{-1}$.

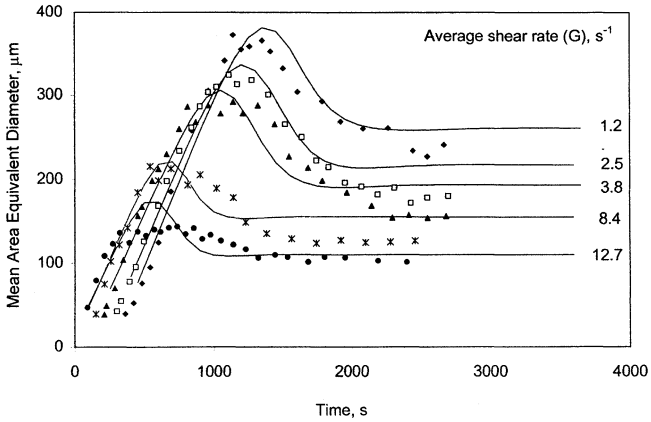

Figure 6. Model prediction vs. experimental data for growth kinetics of asphaltene aggregates under shear at toluene to heptane solvent ratio of 1:15 and particle concentration of 12.8 mg/L.

Solid curves are drawn from the model.

higher particle concentration in the solution. Therefore, a behavior similar to that in Figure 4 is found, that is, lower toluene-to-heptane ratio provides a faster aggregation rate. Although a large variation in the maximum aggregate size is observed, there is a smaller difference in the steady-state floc size for different solvent compositions. Hence, for a fixed stirring speed, increasing the ratio of heptane in the solution greatly enhanced the aggregation rate and increased the steady-state floc size.

Theoretical Modeling

Determination of number concentration for primary asphaltene particles

During an experimental run, the first few captured images at the beginning, or, at that particular time, provided the size distribution of the primary asphaltenes particles. Assuming the primary particles to be spherical, the volume distribution of the primary particles could be determined. At the end of the experiment, the asphaltenes aggregates were filtered and dried in a vacuum oven dryer at 23 kPa absolute pressure and 22°C (room temperature) to determine the mass of the precipitated solid asphaltenes particles. Assuming a specific gravity of 1.2 for solid asphaltenes (Yarranton, 1997), the volume of the primary asphaltenes particles was calculated. Since the well-mixed suspension is homogeneous at the beginning, the size distribution of primary particles from captured images is assumed to be the same for the entire suspension. Hence, the initial number concentration of primary asphaltenes particles in the solution can be calculated.

Comparison of model and experiment

Given an initial distribution of particles, Eq. 4 was solved using a finite difference scheme for each of the 31 size classes until a steady-state size is reached. It can be observed from Eqs. 3, 7, 9–11, and 13 that, except for the breakup rate coefficient b and the porosity of the aggregates ϵ, other model parameters (that is, V_i, d_i, N_i, $\beta_{i,j}$, and $\Gamma_{i,j}$) can be obtained from experimental conditions. Simulations were conducted for different values of G, φ, and X_s.

In Figure 6, model predictions for asphaltenes aggregate growth as a function of shear rate are represented for the asphaltenes volume fraction $\phi = 10.8 \times 10^{-6}$, corresponding to an initial number concentration of asphaltene particles equal to $N_1 = 3.0 \times 10^4$, $N_2 = 1.8 \times 10^4$, and $N_3 = 0.5 \times 10^4$ cm^{-3}. In the model, the porosity of the aggregates ϵ and the breakup coefficient b are used as adjustable parameters and it is intuitive to represent the variations of ϵ and b with shear rate G. Values of ϵ and b are determined by matching the model predicted floc mean diameter with the experimental data for the aggregation of primary asphaltene particles at various shear rates $G = 1.2 \sim 12.7\ s^{-1}$. In Figures 7 and 8, the variations of the fitting parameters b and ϵ with G are represented. In this case, a power relationship, $b = b'G^y$, and a linear relationship $\epsilon = -aG + c$, provide a good fit for the experimental data. The parameters b', y, a, and c are determined by regression analysis of ϵ and b as functions of G. In

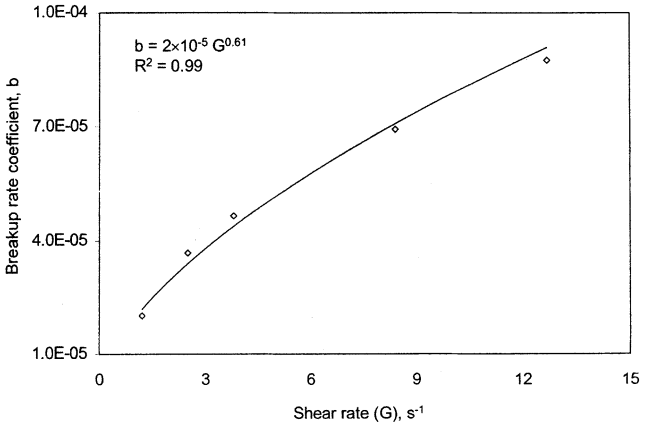

Figure 7. Relationship between the breakup rate coefficient b and the shear rate G at the particle volume fraction $\varphi = 10.8 \times 10^{-6}$.

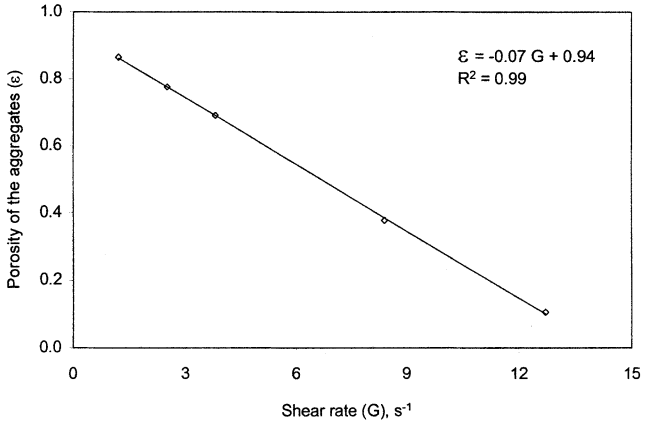

Figure 8. Relationship between the porosity of the aggregates ϵ and the shear rate G at the particle volume fraction $\varphi = 10.8 \times 10^{-6}$.

Figure 6, the results predicted by the model with $b' = 2 \times 10^{-5}$, $y = 0.61$, $a = 0.07$, and $c = 0.94$ are compared to the experimental data over the whole range of G.

In Figure 9, model predictions with the predetermined fitting parameters for asphaltenes aggregate growth at different particle concentrations are represented with and without breakup. For the case of no breakage, b is set to zero. Without breakage, asphaltene aggregates continue to grow monotonically up to a given "stable" size. A maximum does not appear in the aggregate diameter vs. time curve by setting the breakage term to zero. The maximum in the aggregate diameter vs. time is the result of a competition between aggregate growth and breakage. It can be observed that fragmentation greatly affects the average size of the flocs, which is clear from the greater difference between the larger floc size predicted by the model without breakup and the steady-state floc size with breakup.

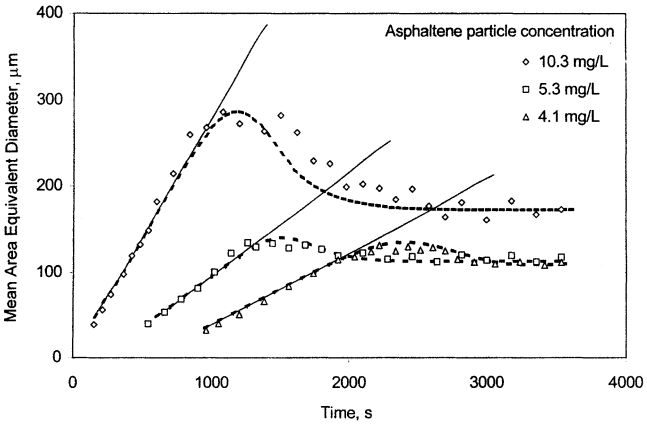

Figure 9. Model prediction vs. experimental data for growth kinetics of aggregates at $G = 2.5\ s^{-1}$ and at different concentrations of asphaltene particles.

Curves are drawn from the model. Solid lines: without breakage at all asphaltene particle concentrations, and dashed lines: with breakage for all asphaltene particle concentrations.

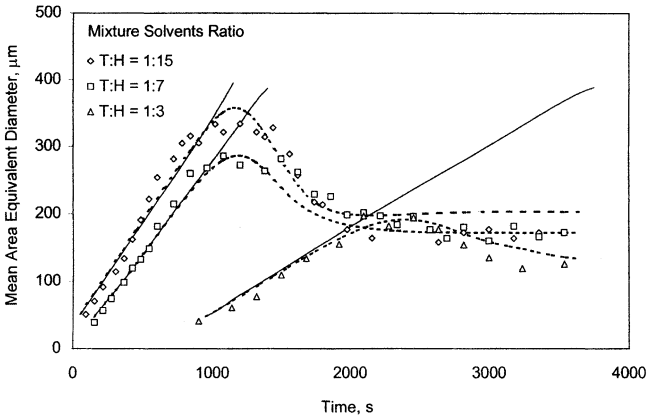

Figure 10. Model prediction vs. experimental data for growth kinetics of asphaltene aggregates at $G = 2.5\ s^{-1}$ and at different ratios of toluene to heptane in solution.

Curves are drawn from the model. Solid lines: without breakage at all solvent compositions, and dashed lines: with breakage for all solvent compositions.

For the case of asphaltene concentration of 10.3 mg/L, there is a larger difference between the attained maximum aggregate size and the steady-state size due to floc restructuring or fragmentation. Whereas in the case of lower asphaltene concentrations, this effect is less noticeable. Hence, it can be inferred that, by reducing the asphaltenes concentration in the solution, the strength of the flocs is increased and they become less susceptible to restructuring or breakage.

In Figure 10, model predictions including breakup and without breakup are represented for asphaltene aggregates growth at different solvent compositions. Again, for the case of no breakage $b = 0$. It is clear from the plots of both Figure 9 and Figure 10 that the initial aggregate growth is not affected by breakage where the mean aggregate diameter increases with time at the same rate whether aggregate breakage is present or not. However, the steady-state aggregate size is affected by breakage. This is especially true when there is a significant maximum in the aggregate size. It can be observed from model results that the solvent composition has a dominant effect on the kinetics of floc growth and the magnitude of aggregate breakup-restructuring, but no significant impact on the final steady-state floc size (see Figure 10).

The two parameters b' and y can be related to the strength of the floc, which depends on flocculants type and concentration, surface properties of the primary particles, floc structure, and suspension medium. All of these factors need to be related to the values of b' and y in order to provide a more mechanistically based description of the floc breakup kinetics. This work also confirms that a simple power law description (Eq. 11) is a useful kinetic model of floc breakup. However, the breakup rate coefficient b is found to be independent of asphaltenes particle concentration φ, and toluene-to-heptane ratio in the solution X_s, at least for present conditions. In the experimental regime, the range for particle volume fraction is about $3.4 \sim 10.8 \times 10^{-6}$, and the solution can be considered very dilute. Hence, b is found to be constant with φ though the number of collisions and the rate of nonlinear breakup increase with higher φ.

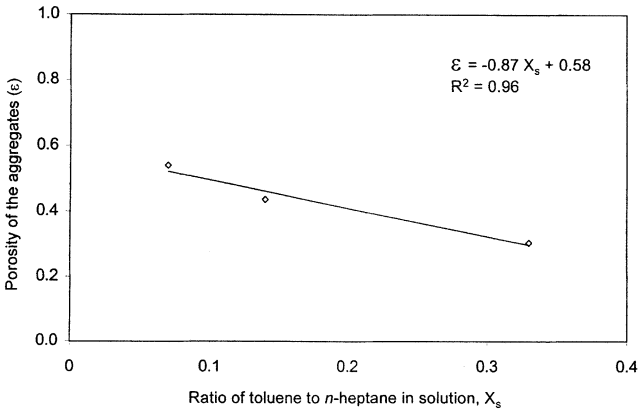

Figure 11. Relationship between the porosity of the aggregates ϵ and the ratio of toluene to *n*-heptane in the solution X_s at the shear rate $G = 2.5\ s^{-1}$.

On the other hand, the porosity of the aggregates ϵ is found to be independent of φ, but shows a weak dependence on X_s. This is due to the fact that the ratio of toluene to heptane in the solvent X_s determines the solubility of asphaltenes particles. At lower toluene-to-heptane ratio, asphaltenes become less soluble in the solution and larger aggregates are formed. However, these aggregates are more susceptible to restructuring-breakage due to their loosely bound structures (Figure 10). Accordingly, a higher porosity is found with decreasing X_s (Figure 11).

Conclusions

This article provides new information on the kinetics of asphaltenes flocculation in the model system. It demonstrates the use of a population balance approach to describe the flocculation phenomena in organic solvents. An experimental study was carried out on the effects of shear rate, particle concentration, and solvent type or composition during aggregation of primary asphaltene particles. The dynamic evolution of asphaltene aggregates growth was monitored by image analysis of the digitized images. Asphaltenes seem to be unique in terms of forming a maximum in the floc size evolution. After a certain period of time, the floc size distribution reached a steady-state size distribution as a result of the competition between aggregation and fragmentation. Increased shear enhanced the aggregation rate as determined from image analysis. The average steady-state floc size always decreased with increasing shear. Increasing the asphaltenes concentration or reducing the ratio of toluene to heptane in the solution increased the floc growth rate and the steady-state floc size.

A population balance model is used in order to understand the dynamics of the aggregation/fragmentation process. The model uses two independent parameters: the porosity of the aggregates ϵ and the breakup coefficient for shear fragmentation b. The parameter ϵ depends on flow characteristics (that is, shear rate G) and solvent composition (X_s). The parameter b was found to depend on the shear rate (G). The relations $b = b'G^y$ and $\epsilon = -aG + c$ fit well with the experimental data. The value of b was found independent of φ in the experimental regime for very dilute suspension.

From a commercial viewpoint, the present study provides information on the significance of shear rate, particle concentration and solvent composition in asphaltenes floc formation, which are essential for proper process design and material handling.

Acknowledgments

We would like to express our gratitude to the Alberta Department of Energy and Albian Sands Energy Inc. for financial support to this project.

Literature Cited

Andersen, S. I. and K. S. Birdi, "Aggregation of Asphaltenes as Determined by Calorimetry," *J. Colloid Interf. Sci.*, **142**, 497 (1991).
Austin, L. G., "A Review: Introduction to the Mathematical Description of Grinding as a Rate Process," *Powd. Tech.*, **5**, 1 (1971).
Boadway, J. D., "Dynamics of Growth and Breakage of Alum Floc in Presence of Fluid Shear," *J. Env. Eng. Div.: Proc. ASCE*, **104**, 901 (1978).
Bouyer, D., A. Line, A. Cockx, and Z. Do-Quang, "Experimental Analysis of Floc Size Distribution and Hydrodynamics in a Jar-Test," *Chem. Eng. Res. Des.*, **79**, 1017 (2001).
Burban, P. Y., W. Lick, and J. Lick, "The Flocculation of Fine-Grained Sediments in Estuarine Waters," *J. Geophys. Res.*, **94**, 8323 (1989).
Burya, Y. G., I. K. Yudin, V. A. Dechabo, V. I. Kosov, and M. A. Anisimov, "Light-scattering Study of Petroleum Asphaltene Aggregation," *Applied Optics*, **40**(24), 4028 (2001).
Chen, W., R. R. Fisher, and J. C. Berg, "Simulation of Particle size Distribution in an Aggregation-Breakup Process," *Chem. Eng. Sci.*, **45**, 3003 (1990).
Cummins, P. G., E. Staples, B. Millen, and J. Penfold, "A Couette Shear Flow Cell for Small-Angle Neutron Scattering Studies," *Meas. Sci. Technol.*, **1**, 179 (1990).
Drushel, H. V., and W. W. Schultz, "Effects of Solvents and Temperature on the Separation of Asphaltenes by Gel-permeation Chromatograpy," Abstracts of Papers of the American Chemical Society, *Second Chemical Congress of North American Continent*, **180**, 148 (1980).
Elimelech, M., J. Gregory, X. Jia, and R. A. Williams, *Particle Deposition and Aggregation: Measurement, Modelling and Simulation*, Butterworth-Heinemann Ltd, Oxford (1995).
Friedlander, S. K., *Smoke, Dust, and Haze*, Wiley, New York (1977).
Gregory, J., "The Density of Particle Aggregates," *Wat. Sci. Technol.*, **36**(4), 1 (1997).
Gregory, J., and Li, G. B., "Flocculation and Sedimentation of High-Turbidity Waters," *Water. Res.*, **25**(9), 1137 (1991).
Han, M. Y., and D. F. Lawler, "The (relative) Insignificance of G in flocculation," *J. Am. Water Works Assoc.*, **84**, 79 (1992).
Higashitani, K., K. Yamauchi, Y. Matsuno, and G. Hosokawa, "Kinetic Theory of Shear Aggregation for Particles in a Viscous Fluid," *J. Chem. Eng. Japan*, **15**, 299 (1982).
Hounslow, M. J., R. L. Ryall, and V. R. Marshall, "A Discretized Population Balance for Nucleation, Growth, and Aggregation," *AIChE J.*, **34**, 1821 (1988).
Jiang, Q., and B. E. Logan, "Fractal Dimensions of Aggregates Determined from Steady state Size Distributions," *Environ. Sci. Technol.*, **25**(12), 2031 (1991).
Kapur, P. C., "Self-Preserving Size Spectra of Comminuted Particles," *Chem. Eng. Sci.*, **27**, 425 (1972).
Kusters, K. A., S. E. Pratsinis, S. G. Thoma, and D. M. Smith, "Ultrasonic Fragmentation of Agglomerate Powders," *Chem. Eng. Sci.*, **48**, 4119 (1993).
Landgrebe, J. D., and S. E. Pratsinis, "A Discrete-Sectional Model for particulate production by Gas-Phase Chemical Reaction and Aerosol Aggregation in the Free-Molecular Regime," *J. Colloid Interf. Sci.*, **139**, 63 (1990).

Long, R. B., "The Concept of Asphaltenes," *Adv. Chem. Ser.*, **195**, 48 (1981).
Long, Y., T. Dabros, and H. Hamza, "Stability and Settling Characteristics of Solvent-Diluted Bitumen Emulsions," *Fuel*, **81**, 1945 (2002).
Mack, C. J., "Colloid Chemistry of Asphalts," *J. Phys. Chem.*, **36**, 2901 (1932).
Masliyah, J. H., "Electrokinetic Transport Phenomena," Pub. No. 12, AOSTRA, Edmonton (1994).
Meakin, P., "Fractal Aggregates," *Adv. Coll. Int. Sci.*, **28**, 249 (1988).
Mishra, V., S. M. Kresta, and J. H. Masliyah, "Self-Preservation of the Drop Size Distribution Function and Variation in the Stability Ratio for Rapid Coalescence of a Polydisperse Emulsion in a Simple Shear Field," *J. Colloid Interf. Sci.*, **197**, 57 (1998).
Mousa, H., and T. G. M. van de Ven, "Stability of Water-In-Oil Emulsions in Simple Shear Flow 1. Determination of the Orthokinetic Coalescence Efficiency," *Colloids Surf.*, **60**, 19 (1991).
Oles, V., "Shear-Induced Aggregation and Breakup of Polystyrene Latex Particles," *J. Colloid Interf. Sci.*, **154**, 351 (1992).
Pandya, J. D., and L. A. Spielman, "Floc Breakage in Agitated Suspensions: Theory and Data Processing Strategy," *J. Colloid Interf. Sci.*, **90**, 517 (1982).
Parker, D. S., W. J. Kaufman, and D. Jenkins, "Floc Breakage in Turbulent Flocculation Processes," *J. San. Eng. Div.: Proc. ASCE*, **98**, 79 (1972).
Pfeiffer, J. P., and R. N. J. Saal, "Asphaltic Bitumen as Colloid System," *J. Phys. Chem.*, **44**, 139 (1940).
Rogacheva, O. V., R. N. Rimaev, V. Z. Gubaidullin and D. K. Khakimov, "Study of Surfactant Activity of Asphaltenes in Petroleum Residues," *Kolloid. Zh.,*, **42**(3), 586 (1980).
Serra, T., and X. Casamitjana, "Effect of the Shear and Volume Fraction on the Aggregation and Breakup of Particles," *AIChE J.*, **44**(8), 1724 (1998).
Shue, E. Y., M. M. De Tar, D. A. Storm, and S. J. DeCanio, "Aggregation and Kinetics of Asphaltenes in Organic Solvents," *Fuel*, **71**, 299 (1992).
Sheu, E. Y., and D. A. Storm, "Colloidal Properties of Asphaltenes in Organic Solvents," *Asphaltenes - Fundamentals and Applications*, E. Y. Sheu and O. C. Mullins, eds., Plenum Press, New York (1995).
Smoluchowski, M., "Versuch Einer Mathematischen Theorie der Koagulations Kinetis Kolloider Losungen," *Z. Physik. Chem.*, **92**, 129 (1917).
Speight, J. G., *Fuel Science and Technology Handbook*, Marcel Dekker, New York, pp. 1193 (1990).
Spicer, P. T., and S. E. Pratsinis, "Coagulation and Fragmentation: Universal Steady State Particle Size Distributions," *AIChE J.*, **42**, 1612 (1996).
Yarranton, H. W., "Asphaltene Solubility and Asphaltene Stabilized Water-in-Oil Emulsions," PhD Thesis, University of Alberta, Dept. of Chemical and Materials Engineering, (1997).
Yen, T. F., and G. V. Chilingarian, ed., *Asphaltenes and Asphalts, 1*, Elsevier, Amsterdam (1994).
Yudin, I. K., G. L. Nikolaenko, E. E. Gorodetskii, E. L. Markhashov, V. A. Agayan, J. V. Sengers and M. A. Anisimov, "Crossover Kinetics of Asphaltene Aggregation in Hydrocarbon Solutions," *Physica A*, **251**, 235 (1998).

Manuscript received May 24, 2002, and revision received Jan. 23, 2003.